Flow-Accelerated Corrosion Modelling of CANDU Outlet Feeders

*O. Silpsrikul**

*Chemical Engineering, University of New Brunswick, PO Box 4400, Fredericton, NB E3B 5A3

Abstract

The primary heat transport system in CANDU reactors is composed of the zirconium alloy in-core components, the carbon steel out-core piping and the Alloy 800 steam generator tubing. The flow-accelerated corrosion (FAC) occurring in the carbon steel outlet feeders at 310°C, because of the undersaturated in dissolved iron there and the high flow rates, dominates and loads the system with magnetite. The FAC is modelled from corrosion mechanisms as the fundamental basis, taking account of electrochemical corrosion potential, oxide film precipitation and dissolution, mass transfer and flow-induced erosion of oxide particles. Good agreement with measurements is obtained.

Introduction

In CANDU-6 reactors, the primary heat transport (PHT) circuit is composed of zirconium alloy in-core components, the SA 106-B carbon steel feeder piping, and the Alloy 800 steam generator tubing. The heavy water (D_2O), utilized as a coolant in the PHT system, flows in the inlet feeders at 265°C to the reactor core to remove heat generated at the reactor core. Subsequently, its temperature is raised to 310°C when leaving the reactor core. The heat in the coolant is utilized to produce steam at the steam generators; therefore, the temperature of the coolant is lowered to 265°C when leaving the steam generators and returning to the inlet feeders.

The coolant is maintained at a constant pH_A, the apparent pH of D_2O calibrated with H_2O solution, of 10.3 to 10.8 by lithium hydroxide addition. In order to minimize dissolved oxygen, 3 to 10 mL/kg of hydrogen gas is added in the coolant. The velocity of the coolant in the inlet and outlet feeders is in the range of 12-17 m/s.

In 1996 at Point LePreau, the failure of outlet feeder S08 caused it s removal and its subsequent examination let to flow-accelerated corrosion being considered the major phenomenon in the outlet feeders. The root cause was undersaturation with dissolved iron in the coolant and high fluid velocity. The work presented here is an attempt to describe the phenomenon of corrosion in the outlet feeders through mathematical modelling based on the fundamental principles of corrosion with an electrochemical aspect.

Corrosion Mechanism

The corrosion reaction is composed of one oxidation reaction and one reduction reaction on the metal surface as shown in equations 1 and 2, respectively:

$$Fe \rightarrow Fe^{2+} + 2e^{-} \tag{1}$$

$$2H^{+} + 2e^{=} \leftrightarrow H_2 \tag{2}$$

Ferrous iron from equation 1 is hydrolyzed to ferrous hydroxide as indicated in equation 3, where b is 1, 2, or 3. It is known that $Fe(OH)_2$ is the major species under alkaline and high temperature based on Tremaine and LeBlanc's work [1980].

$$Fe^{2+} + bH_2O \leftrightarrow Fe(OH)_b^{2-b} + bH^+ \tag{3}$$

A hypothetical thin gap between the metal surface and metal-oxide interface is assumed since the corrosion reaction and oxide formation occur separately, depicted in figure 1.

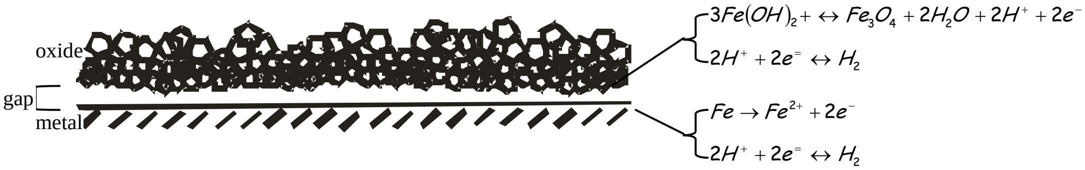

Figure 1. Hypothetical gap and reactions on the metal surface and the metal-oxide interface

On the metal-oxide interface, similarly to the metal surface, there are there are coupled oxidation and reduction reactions; the magnetite formation and hydrogen evolution indicated in equation 4 and 5. Typically, the film is magnetite formed on the carbon steel in high temperature water and under alkaline conditions, as in CANDU feeders,

$$3Fe(OH)_2 + \leftrightarrow Fe_3O_4 + 2H_2O + 2H^+ + 2e^- \tag{4}$$

$$2H^+ + 2e^= \leftrightarrow H_2 \tag{5}$$

The magnetite film is typically duplex which composed of an inner oxide layer and an outer oxide layer [Potter and Mann, 1962]. The inner oxide comprises very fine magnetite as it grows in the confined space on the metal-oxide interface. From Potter and Mann's work [1962], it was found that the inner oxide replaces the volume of the corroded metal. The outer oxide is formed at the oxide-solution interface as it precipitates from solution. Therefore, the outer layer comprises coarse oxide compared with the inner oxide.

Since the inner oxide fills the space of corroded metal, the corrosion rate, CR (in mol/cm^2s), is given by equation 6.

$$\text{Fe in the inner oxide} = CR \times 0.479(1-\phi) \tag{6}$$

where ϕ is porosity.

The remaining dissolved iron from the oxide formation at the metal-oxide interface will diffuse through the oxide film. Diffusion of dissolved iron can be explained by Fick's law:

$$\text{Diffusing dissolved iron} = CR \times (1 - 0.479(1-\phi)) \tag{7}$$

$$CR \times (1 - 0.479(1-\phi)) = \frac{D_{Fe}\phi}{\delta\tau}(C_{mo} - C_{os}) \tag{8}$$

where D_{Fe} is diffusion coefficient of dissolved iron in cm^2/s, δ is the oxide thickness in cm, τ is tortuosity, C_{mo} and C_{os} are concentration of dissolved iron in mol/cm^3 at the metal-oxide interface and at the oxide –solution interface, respectively.

At the oxide-solution interface, the oxide dissolves under iron-undersaturated conditions but precipitates under iron-saturated conditions, as found in the outlet and inlet feeders, respectively. The expression of corrosion rate, equation 9, is obtained from the combination of dissolution/precipitation of oxide, diffusion of dissolved iron, and mass transfer of dissolved iron to the bulk solution.

$$CR = \frac{C_{mo} - \dfrac{\left(k_d A C_{sat} f - k_g C_b\right)}{\left(k_g + k_d A\right)}}{\left(1 - 0.479\left(1 - \phi_i\right)\right)\left(\dfrac{\delta_i \tau}{D_{Fe}\phi_i} + \dfrac{\delta_o \tau}{D_{Fe}\phi_o} + \dfrac{1}{k_g + k_d A}\right)} \tag{9}$$

where C_{sat} is solubility magnetite, C_b is concentration of dissolved iron in the bulk solution, k_g is mass transfer coefficient (cm/s), k_d is magnetite dissolution rate constant (cm/s), A is area factor (1.73), f is particle size factor (1.1), δ_i is the inner oxide thickness, δ_o is the outer oxide thickness (cm), ϕ_i is inner oxide porosity, and ϕ_o is outer oxide porosity.

Flow-Accelerated Corrosion

Flow-accelerated corrosion occurs in a high fluid velocity system, which causes high shear stress, where there are undersaturated conditions. The oxide particle at the oxide-solution interface can be sheared off in high velocity fluid. It takes only a very short time to be sheared off. However, the required time for shearing the particle off not only depends on velocity (*u*), but also depends on particle size (*d*), porosity and dissolution. For the iron-undersaturated condition as in the outlet feeders, required time (t_s) for shearing off is expressed in equation 10.

$$t_s = \frac{sd}{u^2 \phi k_d \left(C_{sat} \times f - C_{os}\right)} \tag{10}$$

Where s is a shearing-off constant

For a saturated system as in the inlet feeders, there is no dissolution mechanism to weaken the oxide film. Therefore, the required time of shearing off does not depend on the magnetite dissolution as indicated in equation 11.

$$t_s = \frac{sd}{u^2 \phi} \tag{11}$$

To estimate the oxide film thickness (δ in μm), equation 12 is applied if there is no outer oxide film and equations 13 and 14 are applied when there is an outer oxide.

$$\delta = \delta_i = \delta_{i,o} + 7.1 \times 10^{-4} CR \cdot \Delta t - k_d A (C_{sat} f - C_{os}) \times 10^{-4} \cdot \Delta t - d \tag{12}$$

If there is outer oxide,

$$\delta_i = \delta_{i,o} + 7.1 \times 10^{-4} CR \cdot \Delta t \tag{13}$$

$$\delta_o = \delta_{o,o} - k_d A(C_{sat} f - C_{os}) \times 10^{-4} \cdot \Delta t - d \tag{14}$$

$$\delta = \delta_i + \delta_o \tag{17}$$

where δ_i is inner oxide thickness, $\delta_{i,o}$ is initial inner oxide thickness, δ_o is outer oxide thickness, $\delta_{o,o}$ is initial outer oxide thickness, and Δt is time increment (second).

Electrochemical Consideration

In general, reactions involving electron transfer produce electric currents. The rate of reaction, corrosion rate for instance, is related to the current by Faraday's law as indicated in equation 15.

$$i_{corr} = CR \cdot nF \tag{15}$$

where i_{corr} is corrosion current, n is number of electron, and F is Faraday's constant (96487 coulomb/mol)

The current can be estimated from the Butler-Volmer equation.

$$i = i_o \left[\exp\left(\frac{\beta nF\left(E - E_{eq}\right)}{RT} \right) - \exp\left(\frac{-(1-\beta) nF\left(E - E_{eq}\right)}{RT} \right) \right] \tag{16}$$

where i_o is exchange current density (Amp/cm^2), β is transfer coefficient, E is local potential (volt), E_{eq} is equilibrium potential (volt), R is Gas constant (8.134 J/mol K) and T is absolute temperature

The equilibrium constant can be obtained from the Nernst equation as indicated in equation 17 and the exchange current density can be estimated from equation 19.

$$E_{eq} = E^o + \frac{RT}{nF} \ln \frac{a_{Ox}}{a_{\mathrm{Re}}} \tag{17}$$

$$Ox + ne^- = \mathrm{Re} \tag{18}$$

Based on equation 18,

$$i_o = k_f C_{Ox} \exp\left(-(1-\beta) nFE_{eq} / RT\right) = k_b C_{\mathrm{Re}} \exp\left(\beta nFE_{eq} / RT\right) \tag{19}$$

where E^o is standard potential, a_{Ox} is activity of species in oxidized side, a_{Re} is activity of species in reduced side, C is concentration in mol/cm^3, and k_f and k_b are the reaction rate constants of forward and backward reaction, respectively.

From equations 16, 17, and 19, the potential at the metal-oxide interface and at the oxide-solution interface are obtained. Both potentials affect the concentration of hydrogen ion across the oxide film via the Nernst-Planck equation [Cussler, 1984]. Moreover, the local potential has the effect on the dissolution rate constant as indicated in equation 21.

$$\left[H^+\right]_{mo} = \left[H^+\right]_{os} \frac{1 - F\left(E_{mo} - E_{os}\right)}{RT} \tag{20}$$

$$k_d^{'} = k_d \exp\left(-\left(1-\beta\right)nFE / RT\right) \tag{21}$$

The equilibrium concentration of dissolved iron, or solubility, at the oxide-solution interface, which affects dissolution/precipitation on the oxide surface, is adjusted by the Nernst equation (equation 17) and the potential at the oxide-solution interface.

Results and Discussion

With the combination of above the mechanisms and the effects of electrochemical potential, the predicted corrosion rate and oxide film thickness after exposed in the system 10,000 hours are consistent with the plant data. The corrosion rate of outlet feeder named S08, at pH 10.2 and fluid velocity of 16 m/s, is 110 μm/a with an oxide film 0.8 μm thick. The estimated potential is -970 mV and -700 mV at the metal-oxide interface and at the oxide-solution interface, respectively. The corrosion potential or potential at the metal-oxide interface should be lower than -900 mV, based on a Pourbaix diagram of the iron system at 310°C constructed from thermodynamic data [Beverskog and Puigdomenech, 1996] and expressions [Shock and Helgeson, 1988; Shock, Helgeson, and Sverjensky, 1989; Archer and Wang, 1990] to estimate some thermodynamic parameters at elevated temperature.

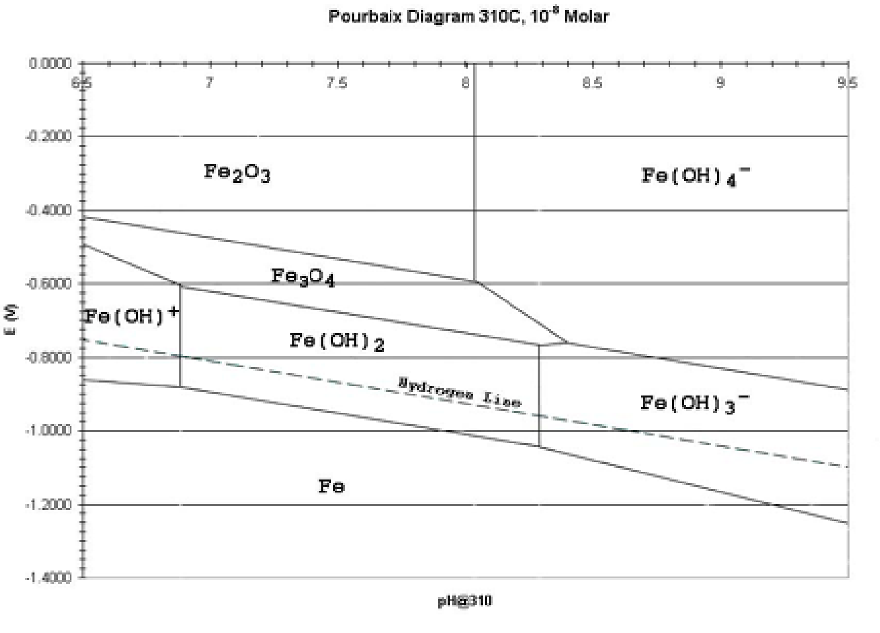

Figure 2. Pourbaix diagram of iron-water system at 310°C, 10^{-8} molar

The potential affects the concentration of hydrogen ion at the metal surface and it was found to be 1.20×10^{-7} mol/kg and the hydrogen ion concentration at the oxide-solution interface is 1.84×10^{-8} mol/kg. The concentrations of dissolved iron at the metal-oxide interface and at the oxide-solution interface are

1.37×10-7 mol/kg and 3.64×10^{-8} mol/kg, respectively. However, it was found that the computed electrochemical solubility of magnetite is very high, 1.4×10^{-6} mol/kg after 10,000 exposure hours. This is almost 100 times the initial solubility and is worth further investigation.

In this work, the effect of pH was also investigated. The results are shown in figures 3 and 4.

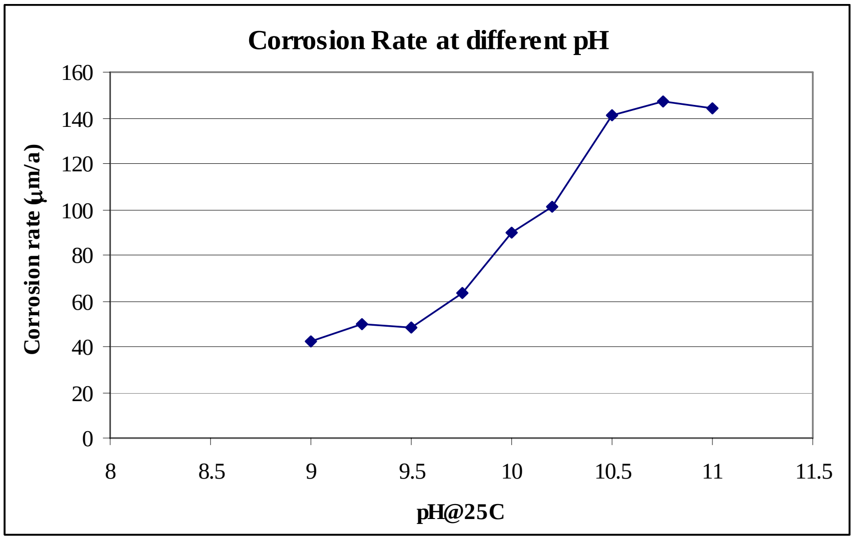

Figure 3. Corrosion rate at different pH

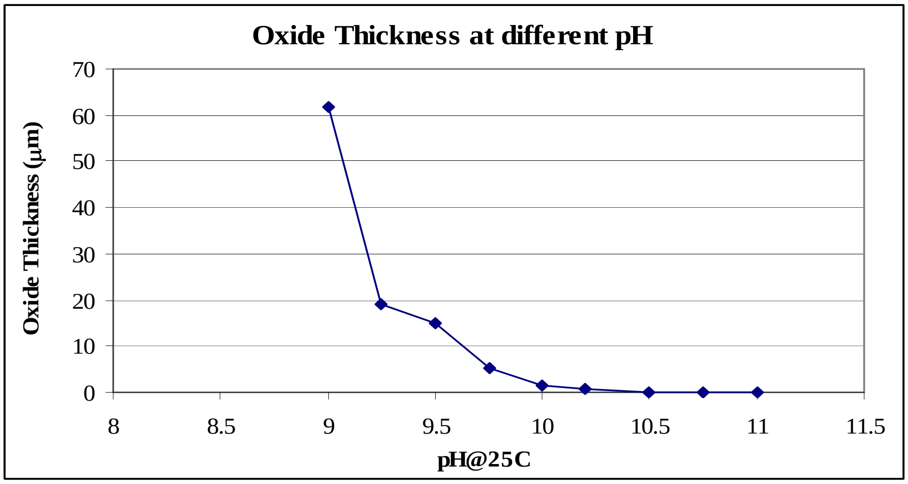

Figure 4. Oxide thickness at different pH

From figures 3 and 4, it was found that corrosion rate increased with pH in the pH range of 9-11. The oxide thickness decreases when pH increases. The thicker oxide, the less the corrosion rate since magnetite is the protective oxide and the thick film causes a barrier to mass transport.

Conclusion

The predicted corrosion rate and thickness of the oxide film are in a good agreement with measurements on a removed feeder. The other parameter values such as potentials, concentrations of hydrogen ion, are concentrations of dissolved iron, etc., are reasonable. However, more investigations on the equilibrium concentration of dissolved iron or magnetite are interesting for future work.

It can be concluded that in the range of pH from 9 to 11, the higher the pH, the greater the corrosion rate and the thinner the oxide film.

Acknowledgement

I thank Dr. D.H. Lister and Dr. F.R. Steward, my supervisors, for all suggestions. Comments and suggestions from Dr. G. Villemure, Dr. N. Susak, and Dr. W. Cook are gratefully acknowledged.

Reference

Archer, D.G., and Wang, P. (1990). The Dielectric Constant of Water and Debye-Huckel Limiting Law Slopes. Journal of Phys. Chem. Ref. Data, 19(2)

Beverskog, B., and Puigdomenech, I. (1996). Revised Pourbaix Diagrams for Iron at 25-300C, Corrosion Science, 38(12), 2121-2135.

Cussler, E.L., (1st edition). 1984. Diffusion Mass Transfer in Fluid System. New York: Cambridge University Press.

Potter, E.C., and Mann, G.M.W. (1962). Oxidation of mild steel in high-temperature aqueous systems. First International Congress on Metallic Corrosion, Butterworth, London.

Shock, E.L., and Helgeson, H.C. (1988). Calculation of the Thermodynamic and Transport Properties of Aqueous Species at High Pressures and Temperatures: Correlation Algorithms for Ionic Species and Equation of State Predictions to 5 kb and 1000 C. Geochimica et Cosmochimica Acta, 52, 2009-2036.

Shock, E.L., Helgeson, H.C., and Sverjensky, D. (1989). Calculation of the Thermodynamic and Transport Properties of Aqueous Species at High Pressures and Temperatures: Standard Partial Molal Properties of Inorganic Neutral Species. Geochimica et Cosmochimica Acta, 53, 2157-2183.

Tremaine, P.R., and Leblanc, J.C. (1980). The solubility of magnetite and the hydrolysis and oxidation of Fe^{2+} in water at 300°C. Journal of Solution Chemistry, 9(6), 415-442.